

AFRL-ML-WP-TP-2006-451

**SIMULATION OF RECURRING
AUTOMATED INSPECTIONS ON
PROBABILITY-OF-FRACTURE
ESTIMATES (PREPRINT)**



**B.D. Shook, H.R. Millwater, M.P. Enright, S.J. Hudak, Jr., and
W.L. Francis**

APRIL 2006

Approved for public release; distribution is unlimited.

STINFO COPY

If this work is published, the publisher may assert copyright. This work was funded by Department of the Air Force Contract F33615-03-2-5203. The U.S. Government has for itself and others acting on its behalf an unlimited, paid-up, nonexclusive, irrevocable worldwide license to use, modify, reproduce, release, perform, display, or disclose the work by or on behalf of the U.S. Government.

**MATERIALS AND MANUFACTURING DIRECTORATE
AIR FORCE RESEARCH LABORATORY
AIR FORCE MATERIEL COMMAND
WRIGHT-PATTERSON AIR FORCE BASE, OH 45433-7750**

REPORT DOCUMENTATION PAGE				<i>Form Approved</i> OMB No. 0704-0188	
The public reporting burden for this collection of information is estimated to average 1 hour per response, including the time for reviewing instructions, searching existing data sources, gathering and maintaining the data needed, and completing and reviewing the collection of information. Send comments regarding this burden estimate or any other aspect of this collection of information, including suggestions for reducing this burden, to Department of Defense, Washington Headquarters Services, Directorate for Information Operations and Reports (0704-0188), 1215 Jefferson Davis Highway, Suite 1204, Arlington, VA 22202-4302. Respondents should be aware that notwithstanding any other provision of law, no person shall be subject to any penalty for failing to comply with a collection of information if it does not display a currently valid OMB control number. PLEASE DO NOT RETURN YOUR FORM TO THE ABOVE ADDRESS.					
1. REPORT DATE (DD-MM-YY) April 2006		2. REPORT TYPE Journal Article Preprint		3. DATES COVERED (From - To) N/A	
4. TITLE AND SUBTITLE SIMULATION OF RECURRING AUTOMATED INSPECTIONS ON PROBABILITY-OF-FRACTURE ESTIMATES (PREPRINT)				5a. CONTRACT NUMBER F33615-03-2-5203	
				5b. GRANT NUMBER	
				5c. PROGRAM ELEMENT NUMBER 62102F	
6. AUTHOR(S) B.D. Shook and H.R. Millwater (University of Texas at San Antonio) M.P. Enright, S.J. Hudak, Jr., and W.L. Francis (Southwest Research Institute)				5d. PROJECT NUMBER 4347	
				5e. TASK NUMBER 27	
				5f. WORK UNIT NUMBER 02	
7. PERFORMING ORGANIZATION NAME(S) AND ADDRESS(ES) <div style="display: flex; justify-content: space-between;"> <div style="width: 45%;"> University of Texas at San Antonio 6900 N. Loop 1604 West San Antonio, TX 78249 </div> <div style="width: 45%;"> Southwest Research Institute 6220 Culebra Road P.O. Drawer 28510 San Antonio TX 78228-0510 </div> </div>				8. PERFORMING ORGANIZATION REPORT NUMBER	
9. SPONSORING/MONITORING AGENCY NAME(S) AND ADDRESS(ES) Materials and Manufacturing Directorate Air Force Research Laboratory Air Force Materiel Command Wright-Patterson AFB, OH 45433-7750				10. SPONSORING/MONITORING AGENCY ACRONYM(S) AFRL-ML-WP	
				11. SPONSORING/MONITORING AGENCY REPORT NUMBER(S) AFRL-ML-WP-TP-2006-451	
12. DISTRIBUTION/AVAILABILITY STATEMENT Approved for public release; distribution is unlimited.					
13. SUPPLEMENTARY NOTES If this work is published, the publisher may assert copyright. This work was funded by Department of the Air Force Contract F33615-03-2-5203. The U.S. Government has for itself and others acting on its behalf an unlimited, paid-up, nonexclusive, irrevocable worldwide license to use, modify, reproduce, release, perform, display, or disclose the work by or on behalf of the U.S. Government. This paper has been submitted to Structural Health Monitoring, published by Sage Publications. PAO Case Number: AFRL/WS 06-0791, 22 Mar 2006.					
14. ABSTRACT On-board sensors that can detect and size a crack in a structural component are being developed and will be deployed to enhance structural health monitoring and prognosis. This research examines the simulation of recurring automated inspection resulting from simulated on-board "crack" sensors, and their potential effect on reducing the probability-of-fracture of structural components. The concept of a probability of detection (POD) curve is used to characterize the performance of the sensor, as done for traditional inspections. However, we assert that recurring inspections for an automated system should be modeled as dependent with respect to the first inspection due to the largely repeatable aspects of the sensor and data collection system. This assertion has a large effect on the computed probability of detecting a crack and alleviates the substantial over prediction of sensor efficacy generated using the assumption of independent inspections for automated systems. Furthermore, it is demonstrated that the fundamental feature that determines the efficacy of a recurring automated on-board sensor is the probability of detecting a crack of critical size, i.e., the size that will cause fracture, and this feature is by and large separate from the shape of the POD curve. This information can be used to determine the required accuracy of an on-board automated inspection to achieve a specified reliability of a structural component. The methodology is demonstrated using fatigue and fracture of a representative titanium compressor disk from a gas turbine aircraft engine but is applicable to any structural system with recurring automated inspections.					
15. SUBJECT TERMS Crack, sensors, probability of detection (POD) curve, fracture, fatigue					
16. SECURITY CLASSIFICATION OF:			17. LIMITATION OF ABSTRACT: SAR	18. NUMBER OF PAGES 46	19a. NAME OF RESPONSIBLE PERSON (Monitor) Patrick J. Golden 19b. TELEPHONE NUMBER (Include Area Code) N/A
a. REPORT Unclassified	b. ABSTRACT Unclassified	c. THIS PAGE Unclassified			

Simulation of Recurring Automated Inspections on Probability-of-Fracture Estimates

B.D. Shook, H.R. Millwater

University of Texas at San Antonio

6900 N. Loop 1604 West

San Antonio, TX 78249

M.P. Enright, S.J. Hudak, Jr., W.L. Francis

Southwest Research Institute

6220 Culebra Road

San Antonio, TX 78238

Abstract

On-board sensors that can detect and size a crack in a structural component are being developed and will be deployed to enhance structural health monitoring and prognosis. This research examines the simulation of recurring automated inspections resulting from simulated on-board “crack” sensors, and their potential effect on reducing the probability-of-fracture of structural components. The concept of a probability of detection (POD) curve is used to characterize the performance of the sensor, as done for traditional inspections. However, we assert that recurring inspections for an automated system should be modeled as dependent with respect to the first inspection due to the largely repeatable aspects of the sensor and data collection system. This assertion has a large effect on the computed probability of detecting a crack and alleviates the substantial over prediction of sensor efficacy generated using the assumption of independent inspections for automated systems. Furthermore, it is demonstrated that the fundamental feature that determines the efficacy of a recurring automated on-board sensor is the probability of detecting a crack of critical size, i.e., the size that will cause fracture, and this feature is by and large separate from the shape of the POD curve. This information can be

used to determine the required accuracy of an on-board automated inspection to achieve a specified reliability of a structural component. The methodology is demonstrated using fatigue and fracture of a representative titanium compressor disk from a gas turbine aircraft engine but is applicable to any structural system with recurring automated inspections.

Introduction

Direct on-board detection of material defects and subsequent sizing and damage prognosis has the potential to revolutionize the assessment and use of structural systems. This technology will extend current structural health monitoring by providing a much-improved assessment of the state of the material. This assessment, obtained by the coupling knowledge of the loading history of the component with the ability to size, monitor and assess the criticality a defect through well-developed fracture mechanics, provides the necessary information to manage the a fleet of structures and to prognose its current and future health.

The Defense Advanced Research Projects Agency (DARPA) has initiated a “prognosis” effort to develop the technology to make the on-board prognosis of material health a reality. The prognosis program will use advanced, physics-based and data-driven models supplemented by advanced sensors to assess the health of individual weapon systems as they are subjected to damage, stresses, and corrosion during operational use. This capability will enable management and deployment of critical assets based on their real remaining useful life and capability rather than on assumptions. The current focus is for aircraft structures and engines. The anticipated benefit is to double the useful life of gas turbine engine components and increase by five-fold the accuracy of estimating aircraft fatigue life[DARPA News Release,(2003); Larsen, and Christodoulou,(2004); Christodoulou and Larsen,(2004)].

A portion of the DARPA effort is to develop wireless magnetostrictive thin-film sensors for “direct” detection and monitoring of fatigue cracks at elevated temperatures[Hudak, et al.,(2004)]. This technology has the potential to provide the feedback on the material damage state needed to achieve real-time or near real-time prognosis.

Current research summarized in this paper is focused on the probability of detecting a material defect as a function of recurring automated inspections, herein referred to as “continual” inspections. In particular, we attempt to answer questions such as: how much benefit is obtained through the use of on-board sensors that provide continual interrogations of the material? What accuracy of the on-board sensor is required to improve upon the current practice of a single detailed mid-life inspection?

The traditional approach to inspection simulation is to assume each inspection is independent from the previous. This assumption is appropriate for the traditional application of inspections, i.e., different operators, equipment, and location, and widely separated by the time of inspection. Well-established computer models for determining probability-of-fracture (POF) estimates for aircraft structures [Berens, et al.,(1991)]; and gas turbine rotor disks [Leverant, et al.,(2004)] consider infrequent or opportunity inspections, and; therefore, model the inspections as independent.

However, the assumption of independent inspections leads to dramatic predictions of non-realizable efficacy for continual inspections and the results are frequency dependent; almost any size crack can be detected by inspecting more and more frequently. The assumption of independent inspections is severely non-conservative and provides a false estimate of the accuracy of continual inspections.

Conversely, it is asserted and discussed below that continual inspections should not be treated as independent from previous inspections but as dependent; since the same sensor is performing subsequent inspections, the sensitivity of the sensor in detecting the crack should be the same as for previous inspections, or nearly so. Dependant inspections enforce that the sensitivity of a sensor at one inspection is the same at subsequent inspections.

An examination of redundant fluorescent penetrant inspection (FPI) substantiates the fact that repeated inspections should not be treated as independent and that doing so is nonconservative [Erland, (1988)]. In this study, data from a group of specimens are inspected in the same FPI processing situation by two inspectors of approximately the same skill level. The resultant probability-of-detection from both inspections is quantified using data and compared with the independent assumption. The data-based POD is significantly lower than the independent-based POD. As stated, “The fluorescent penetrant inspection process is not independent inspection-

to-inspection and therefore the probability of detection for redundant FPI cannot be obtained by a simple multiplication of probabilities. The correct POD in a multiple inspection system is determined assuming dependence.”

Mathematical bounds are developed that prove that independent and dependent inspections provide the upper and lower bounds, respectively, on the cumulative probability of detecting a defect. That is, assuming dependent inspections is a conservative assumption. Intermediate results can be obtained by correlating the inspections with a correlation coefficient between zero (independent) and one (dependent).

Given the assertion of dependent inspections, it is shown that the efficacy of an on-board sensor is principally determined by the probability of detecting a crack of critical size, (the size of the crack that will fracture the material) and, by and large, unaffected by the shape of the POD curve. This information can be used to: a) determine the effectiveness of implementing a particular sensor on a structural component, or b) determine the necessary design specification a sensor must satisfy to make an implementation effective for component safety and management of the asset.

The concept of a POD curve is still viable for an on-board sensor although it may be developed differently than for traditional inspection systems. The POD curve for a particular on-board sensor will be unknown; therefore, a POD curve for a specific manufacturing and application “process” will most likely be developed. A POD curve for a sensor indicates that not all sensors are manufactured and operate identically; there is variation in the detectability between sensors. For example, the POD for an embedded sensor would be developed based on the manufacturing process of the sensor, the corresponding electronics, and the in situ environment of application. Development of the POD would involve a test article with multiple embedded sensors and a series of cracks of various sizes. Multiple test articles would be used in order to determine the POD as a function of crack sizes. Potentially, in the future, computational methods incorporating the physics of the sensor mechanics, structural mechanics, and probabilistic methods will be used to develop computational POD curves[Rajesh et al., 1993].

The paper is organized as follows. A short description of a probability of detection curve is given, followed by a detailed discussion of the numerical procedure for simulating single and subsequent recurring inspections

using Monte Carlo sampling. This section also includes a discussion and justification for using “dependent” inspections for recurring inspection systems. Mathematical bounds for the cumulative probability of detection are defined next, followed by the equations for evaluating the probability-of-failure, and a methodology for estimating the efficacy of an on-board sensor system. Subsequently, numerical examples are presented that demonstrate the differences in cumulative probability-of-detection as a function of correlation coefficient and the parameters of the POD curve, and finally, a comparison is presented between continual inspections and a more accurate single mid-life depot inspection. The numerical examples used to support the conclusions consider a crack at the bore of a titanium gas turbine disk; however, the technology is not limited to this structural component and is broadly applicable to on-board sensing systems in general.

Inspection Simulation

The accuracy and variability of an inspection system is embodied in the concept of a Probability-of-Detection curve. The POD curve relates the probability of detecting a flaw to the flaw size [Simola and Pulkkinen, (1998)] and is determined through statistical experimentation and calibration involving a sufficiently large number of randomized trials [Berens, 1989]; however, some effort is being made towards “model-assisted” POD development[Rajesh, S. N., Udpa, 1993; Model-assisted working group(2004)]. Factors that affect a POD curve include the physical properties of cracks with the same size (location, orientation to test equipment, etc.), repeatability of the signal response data for a given crack, human factors, differences in inspection hardware, environmental conditions, and surface conditions, among others. An industry accepted ultrasonic POD curve and its derivative are shown in Figure 1. Typical equations used to model POD curves are log-odds, log-logistic, or lognormal distributions[Berens, (1989)].

Simulation of inspections can be accomplished using Monte Carlo sampling. The variation in sensor sensitivity, represented by the POD curve, is simulated through repeated realizations generated from the POD curve. Each realization represents a sensor of a specific sensitivity of detectible crack size (DCS), i.e., a_{DCS} . The sensor represented by realization n will detect all cracks of size larger or equal to its DCS (a_{DCS}) and miss

cracks of smaller size. The realizations, nS_k , are generated independently from a uniform probability distribution and represent $POD({}^na_{DCS})$. ${}^na_{DCS}$ is then generated as

$${}^na_{DCS} = POD^{-1}({}^nS_k) \quad (1)$$

For each realization, the size of the crack at the time of inspection, a_k , is compared against ${}^na_{DCS}$. If

$${}^na_{DCS} \leq a_k \quad (2)$$

the inspection (sensor, equipment, human operator, etc.) is adequately sensitive and the crack is detected; otherwise the crack is missed. An equivalent probability statement is

$$POD({}^na_{DCS}) \leq POD(a_k) \quad (3)$$

and this statement is often used in place of Equation 2 since the inverse operation, Equation 1, is avoided. Sampling is repeated sufficiently such that a converged solution is obtained. A schematic of the procedure using a single sample is shown in Figure 2 for realization n . Note, this approach for generating inspection sensitivities from the POD curve is the same as used for generating independent random variables in general [Millwater and Wirsching, (2003)]

Simulation of Continual Inspections

Frequent, recurring inspections using automated inspection systems are herein called “continual” inspections. Simulation of continual inspections is important in order to determine the efficacy of proposed inspection systems and, ideally, to determine the sensor accuracy necessary to make the automated inspection system worth developing and deploying.

For subsequent inspections, traditionally it is assumed that the inspection process is significantly different from any previous inspections: different inspection equipment, operator, environmental conditions, etc. Therefore, during the inspection simulation, samples representing sensor sensitivity are drawn statistically independent from samples from previous inspections. That is, the samples generated and used from the previous inspection have no effect on the samples generated for subsequent inspections. For example, the first

realization drawn for inspection k is independent from the first realization for inspection $k-1$, i.e., 1S_k is generated independently from $^1S_{k-1}$. If the samples represent inspections performed at significantly different times by different operators, using different equipment etc., then the independent sampling approach is appropriate.

For recurring automated inspections, subsequent inspections involve realizations of the same sensor(s), inspection equipment, and operator. The simulation of an automated inspection system is accomplished by simulating the sensor each time it is actuated. nS_k represents the realization of the n th sensor at the k th inspection and has associated with it a DCS of $^na_{DCS(k)} = POD^{-1}(^nS_k)$. The detectible crack size for subsequent inspections for the *same* sensor should not be significantly different from the detectible crack size at the first inspection, that is $^na_{DCS(k)} \approx ^na_{DCS(1)}$, or, $POD(^na_{DCS(k)}) \approx POD(^na_{DCS(1)})$, and; therefore, $^nS_k \approx ^nS_1$. Stated differently, on the first inspection, the realization nS_1 selects a sensor from the range of all possible values from the sensor manufacturing process and in-situ application, represented by the POD curve. For a subsequent inspection by the same sensor, the sensor has already been selected from the pool of potential values that describe the variation in the inspection process and subsequent sampling only represents the variation between inspections given the same sensor, e.g., environment, electronics. As such, a subsequent realization representing the same sensor should not be generated independently from a realization from the previous inspection since the sensor sensitivities should not be far apart, i.e., $^na_{DCS(k)} \approx ^na_{DCS(1)}$.

In the limiting case, the realizations are dependent, i.e., the variation in the sensitivity for a particular sensor across inspections is zero, $^na_{DCS(k)} = ^na_{DCS(1)}$, or $POD(^na_{DCS(k)}) = POD(^na_{DCS(1)})$, and therefore, $^nS_k = ^nS_1$. Thus, the samples are fully dependent across inspections. Given an initial realization for inspection 1, the same value is used for a particular sensor for all subsequent inspections.

The contrast between simulation of independent and dependent inspections is shown in Figures 3 and 4 for a hypothetical crack growth and inspection scenario. Four inspections are represented with four realizations for each inspection. Each realization is represented by a different symbol (circle, diamond, triangle, square). The continuous line represents $POD(a_k)$.

The differences in the mechanics and the results of the independent and dependent assumptions for continual inspections are dramatic with independent inspections predicting a far larger, perhaps a factor of many times, reduction in POF. As show in Figure 3, for independent inspections, the sensitivity for a particular sensor, say the sensor represented by the red square symbol, will vary dramatically from inspection to inspection; initially not sensitive ($POD=0.85$), then fairly sensitivity ($POD=0.18$), then very sensitive ($POD=0.03$), then very insensitive ($POD=0.97$). Clearly, this modeling assumption is illogical for recurring automated inspections. By contrast, Figure 4 shows that the sensor sensitivity does not change for different inspections, that is, $POD({}^n a_{DCS(k)}) = POD({}^n a_{DCS(1)})$, and; therefore, ${}^n a_{DCS(k)} = {}^n a_{DCS(1)}$.

The reason the modeling assumption of independent inspections over predicts the inspection efficacy is that the defect is assumed found for a sensor realization if at *any time* during the course of inspections $POD({}^n a_{DCS}) \leq POD(a_k)$. That is, for the simulation of one particular sensor, if the samples are generated independent of any previous inspections, the probability of detecting the defect increases dramatically as the number of inspections increase; each realization is highly likely to detect the defect if sufficient inspections are simulated even for very small defects compared to the POD curve. In contrast, samples generated dependently, shown in Figure 4, do not show any increase in the probability of detecting a defect due the frequency of inspection; the increase is only due to the growth of the defect and the corresponding increase in $POD(a_k)$.

In operation, multiple inspections of on-board systems will not be completely repeatable; there will be some variation in sensitivity between inspections due to the sensor electronics, thermal cycling of the sensor, environment, etc., although we expect the variation to be relatively minor compared to the variation represented by the POD curve since this is an “intra-sensor” variation for a particular sensor across inspections, versus an “inter-sensor” variation across sensors. Clearly there will be an underlying mechanism for variations in the sensor sensitivity and a model based on physical effects may be possible. An alternative approach that is straightforward to implement and efficient is to use statistical “correlation” between subsequent sampling realizations during the numerical simulation process; a correlation coefficient of “one” denotes dependent

inspections and a correlation coefficient of “zero” denotes independent inspections. Once nS_1 is generated, nS_k is generated such that $\rho_{1k} = \rho$, where ρ denotes the correlation coefficient and here $0 \leq \rho \leq 1$.

The “sum-of-uniforms” (SOU) method is ideal for efficiently generating correlated realizations[Willemain and Desautels, (1993); et al., Chen]. The sum-of-uniforms method adds uniformly distributed random numbers then transforms the sum to obtain a new uniformly distributed random number with the desired correlation between the original and generated random numbers. The newly generated correlated sample is then used to generate the next value, etc. Using the SOU method, it is simple procedure to generate nS_k given nS_1 such that a desired correlation coefficient, $\rho_{1k} = \rho$, is enforced by continually using the value of nS_1 as the base number in the algorithm. SOU is very fast and requires minimum storage. Thus, realizations for any number of samples and inspections can be easily generated.

Mathematics of Continual Inspections

Multiple inspections can be modeled as a “series” system. That is, the probability of detecting a defect after k inspections is the probability that the crack is detected at inspection 1, or inspection 2, etc. First order bounds based on “dependence” or “independence” of the inspections are given by[Cornell, 1967]

$$\max[POD(a_k)] \leq CPOD(a_{1-k}, k) \leq 1 - \prod_{i=1}^k (1 - POD(a_i)) \quad (4)$$

where POD denotes the parent POD of the sensor process, a_i denotes the crack size at inspection i , k denotes the number of inspections and also inspection k , a_{1-k} denotes dependence on the crack sizes at inspections one through k , and $CPOD$ denotes the cumulative probability of detection, that is, the probability of detecting a defect after k inspections. The lower bound corresponds to dependent inspections and the upper bound corresponds to independent inspections[Millwater & Wirsching,(2003)]. In general, the CPOD is a function of the number of inspections k and the crack sizes at the time of all inspections, a_{1-k} .

Dependent Inspections

If the inspections are fully dependent then the cumulative POD value at inspection k is the POD value of the parent POD for a defect size of a_k , since for all previous inspections the defect is always smaller than at inspection k . This situation is denoted by the lower bound in Equation 4. That is,

$$\max[POD(a_k)] = POD(a_k) = CPOD(a_k) \quad (5)$$

Under this condition, the cumulative POD collapses to the parent POD. The cumulative probability of detecting a crack is *not dependant* on the number of inspections or the size of the crack at previous inspections; it is only dependant on the POD value at the time of inspection k ; the last inspection. Thus, the CPOD increases only as defect size increases and at a rate defined by the parent POD. The probability of detecting a defect does not increase due to multiple inspections, only due to an increase in the defect size.

Independent Inspections

If the inspections are independent, the probability of detecting a crack after k inspections is the probability that the crack is detected at inspection 1, or inspection 2, or ... or inspection k . Mathematically, this is given by

$$CPOD(a_{1-k}, k) = POD(a_k) \bigcup POD(a_{kM1}) \bigcup POD(a_{kM2}) \bigcup \dots \bigcup POD_1(a_1) \quad (6)$$

where a_k indicates the crack size at inspection k , a_{kM1} indicates the size of the crack at one inspection before k , a_{kM2} indicates the size of the crack at two inspections before k , a_1 denotes the size of the crack at the initial inspection, a_{1-k} denotes dependence on the crack sizes at inspections one through k , the symbol \bigcup indicates the “union” operator, $POD(a_k)$ indicates the probability of detecting a crack at inspection k from the parent POD, and $CPOD(a_{1-k}, k)$ indicates the cumulative probability of detecting a crack of size a_k after k inspections.

The cumulative probability of detection is calculated more easily as one minus the probability of not detecting a crack at any inspection. Mathematically, this is

$$CPOD(a_{1-k}, k) = 1 - (1 - POD(a_k)) \bigcap (1 - POD(a_{kM1})) \bigcap \dots \bigcap (1 - POD(a_1)) \quad (7)$$

where the symbol \bigcap indicates the “intersection” operator.

If the probability of detecting a crack at any one inspection is independent from any other inspection, Equation (7) becomes

$$CPOD(a_{1-k}, k) = 1 - (1 - POD(a_k)) \bullet (1 - POD(a_{kM1})) \bullet \dots \bullet (1 - POD(a_1)) \quad (8)$$

where “ \bullet ” indicates multiplication.

Equation (8) is represented by the right hand equality of Equation (4), that is

$$CPOD(a_{1-k}, k) = 1 - \prod_{i=1}^k (1 - POD(a_i)) \quad (9)$$

Therefore, the cumulative probability of detecting a crack at “any time” before and including inspection k , is one minus the product of missing the crack at the current and all previous inspections.

Evaluation of the Probability-of-Fracture

The probability-of-fracture is determined using a probabilistic fatigue analysis to determine a_k , integrated with the inspection simulation process described in previous sections[Leverant et al., (2004); Millwater, et al. (2000)]. Randomness in variables that govern the fatigue process, e.g., initial crack size, stress amplitude, life prediction accuracy, etc., is reflected in the stochastic nature of a_k and can be considered combined with the POD curve. Monte Carlo sampling can be used to address both the random fatigue and the random inspection processes.

For an airframe structure the crack may be removed by repair. A “repair” initial crack size distribution is then used to proceed forward in time [Berens, et al., (1991)]. For engine structures, repair is typically not possible and the simulation removes the disk from service[Leverant, et al., (2004)]. In this case, the POF is monotonically increasing with the number of flight cycles, and the POF without and with inspection are computed as

$$P_{F,woi} \approx \frac{N_{f,woi}}{N} \quad (10)$$

$$P_{F,wi} \approx \frac{N_{f,wi}}{N} \quad (11)$$

where *woi* indicates “without inspection”, *wi* denotes “with inspection”, $N_{f,woi}$ denotes the number of samples that have failed without inspection, $N_{f,wi}$ denotes the number of samples that have failed with inspection, and N denotes the total number of samples. The reduced POF can be determined as

$$P_{F, reduced} = \frac{P_{F, wi}}{P_{F, woi}} = \frac{N_{F, wi}}{N_{F, woi}} \quad (12)$$

The number of failures, and; therefore, the POF's, are a function of the number of flight cycles due to fatigue crack growth.

Estimating the Required Sensor Accuracy for Continual Monitoring

A critical piece of information for designing an on-board inspection system is the required accuracy of the sensor such that continual inspections offer an improvement over the traditional mid-life inspection. Consider a deterministic crack growth analysis that would result in a single representative crack growth curve (cycles versus size) shown in Figure 5. Fracture of the part occurs when a crack reaches the critical size after being missed by the continual inspections.

For dependent inspections, the probability of a crack being missed by all inspections and fracturing the part is given by one minus the POD at the last inspection, i.e., $1 - POD(a_{last})$, where *last* indicates the last inspection before fracture. A sufficient frequency of continual inspections would insure $a_{last} \approx a_{crit}$. As a result, the “reduced” POF is approximately $1 - POD(a_{crit})$. In other words, for the cracks that would cause fracture, the reduced POF is

$$P_{F, reduced} = \frac{P_{F, wi}}{P_{F, woi}} \approx 1 - POD(a_{crit}) \quad (13)$$

and since no cycle values are preferential,

$$P_{F, wi}(M) \approx P_{F, reduced} \cdot P_{F, woi}(M) = [1 - POD(a_{crit})] \cdot P_{F, woi}(M) \quad (14)$$

where M indicates the number of flight cycles. That is, the scale factor, $1 - POD(a_{last})$, can be used to determine $P_{F, wi}(M)$ at any number of cycles.

If the crack growth is non-deterministic, multiple crack growth curves will occur. However, it is still true that a part will fracture only when a crack reaches the critical size after being missed by the continual inspections. If the frequency of continual inspections is sufficient, again $a_{last} \approx a_{crit}$, then Equations 13 and 14 also hold for non-deterministic crack growth.

In practice, the crack size at the last inspection, a_{last} , will be less than a_{crit} and, therefore,

$$P_{F, reduced}^{Actual} \geq P_{F, reduced}^{Theoretical} \quad (15)$$

where $P_{F, reduced}^{Actual}$ indicates the realized reduced POF during numerical application, and $P_{F, reduced}^{Theoretical}$ is given by Equation 13. Thus, $P_{F, reduced}^{Theoretical}$ represents a lower bound to the POF after continual inspections.

The ability of $POD(a_{crit})$ to determine the effectiveness of the sensor in reducing the POF is determined by the value of the crack size at the time of the last inspection, a_{last} , which depends upon the frequency of inspections relative to the crack growth rate near the critical crack size. Thus, a sufficient frequency of inspection would ensure that $P_{F, reduced}^{Actual}$ is close to its theoretical limit of $P_{F, reduced}^{Theoretical}$ and Equations 13 and 14 would be high-quality indicators of the reduced POF due to the particular sensor under consideration. This theoretical limit will be more easily obtained the “flatter” the POD curve at the critical crack size, that is, a POD curve with a small value of slope, $dPOD(a)/da|_{a_{crit}}$ will be less sensitive to the time of the last inspection and vice versa.

Predicting the Reduced POF with Non-Deterministic Critical Crack Size

The previous section outlined the approach for determining the reduced POF due to inspection based solely upon the value of the POD curve at the critical crack size. However, the critical crack size, a_{crit} , may be random due to randomness in stresses or fracture toughness, for example. In this situation, the reduced POF can be computed by integrating over the probability density functions (pdfs) as

$$P_{F, reduced} = 1 - \int POD(a_{crit}(\sigma, K_C)) f_{\sigma} f_{K_C} d\sigma dk_c = 1 - E[POD(a_{crit})] \quad (16)$$

where σ represents stress scatter with pdf f_{σ} , K_C represents fracture toughness with pdf f_{K_C} , and

$E[POD(a_{crit})]$ is the expected value of $POD(a_{crit})$. Equation 16 reduces to Equation 14 if a_{crit} is deterministic.

The effect of a non-deterministic critical crack size is less pronounced the “flatter” the POD curve and more pronounced the “steeper” the POD curve, that is $dPOD(a)/da|_{a_{crit}} = pod(a_{crit})$ determines the sensitivity of the sensor to variations in a_{crit} , where we use the notation pod to indicate the pdf of the POD curve. In effect, a small value, and a large value of $pod(a_{crit})$, indicates that the sensor will not be, and will be, sensitive to variations in a_{crit} , respectively. For example, if the POD curve is flat over the region defined by the range of the pdf, e.g., f_{σ} , and f_{K_C} , then $POD(a_{crit})$ will be nearly constant for the integration given in equation 16, and; therefore, $P_{F, reduced}$ will be minimally affected.

Numerical Examples: Effects of Variations in Inspection Frequency, Correlation, POD Parameters –

The difference in inspection efficacy between an assumption of independent and dependent inspections is dramatic and is a function of a number of parameters, most prominent being the frequency of inspection. A numerical example of a crack in a compressor disk is used as a template to examine various effects. The sum-of-uniforms method is integrated into a probabilistic fatigue analysis program [Leverant, et al., (2004)] to facilitate analyses given an arbitrary correlation coefficient between recurring inspections Shook, et al, (2005)].

The problem consists of a surface crack on the bore of a gas turbine disk. The stress spectra applied to the crack is derived from RPM values versus time obtained from a flight data recorder representative of an Air-to-Ground military mission which contains 115 damage pairs. The initial crack size is a semi-circular defect with an initial crack depth specified by an exponential probability distribution and a 1-to-1 aspect ratio with a mean 0.432 mm (17 mils). The initial crack size distribution is representative of the cracks initiated on holes in compressor disks due to machining. Other initial defect size distributions can be considered without altering the main conclusions. Material properties for a titanium material are used. The material fractures at a critical crack

surface length of approximately 15.24 mm (600 mils) under the applied loading. See Table 1 for a summary of the problem definition.

The POD curve is modeled with a lognormal distribution,

$$POD(A \leq a) = \Phi[\ln(a/\tilde{X})/\sigma_y] \quad (17)$$

where a represents crack size, \tilde{X} is the median, COV is the coefficient of variation, $\sigma_y^2 = \ln[1 + COV^2]$, and Φ represents the standard normal cumulative distribution function. The COV used for the POD curves is chosen as thirty-two percent based on analysis of existing industry ultrasonic POD curves[TRMD final report, (2000)]. (Multiple industry ultrasonic POD curves of varying sensitivity calibrations are available for ultrasonic inspections; remarkably, they all exhibit a COV of approximately thirty-two percent.) Since an on-board crack sensor does not yet exist, the descriptive parameters of the POD curve are speculative but are useful to demonstrate and support conclusions. The median value and COV values for the POD curve are varied to represent sensors of varying sensitivity, as discussed below.

Effects of Changes in Inspection Correlation Coefficient, and POD Sensitivity on the CPOD

Figure 6 shows the effect of various levels of correlation between inspections, with an inspection simulated after each flight. A correlation coefficient of one corresponds to fully *dependent* inspections and a correlation coefficient of zero corresponds to *independent* inspections. As expected, a correlation coefficient of one (dependent continual inspections) shows that the CPOD equals the parent POD, whereas a correlation coefficient of zero (independent continual inspections) shows a dramatic benefit. For example, the CPOD after 1000 flight cycles is approximately 1% and 93% for the for the dependent and independent models, respectively; a ratio of over ninety.

Correlation coefficients between zero and one yield CPOD values between the dependent and independent inspections. The figure shows that even for a correlation coefficient equal to 0.8, a significant improvement in the cumulative probability of detection can be achieved by performing continual inspections. However, since the correlation will not be know a priori, Figure 6 makes it clear that the most conservative estimate for the

benefit achievable with multiple inspections, and the procedure recommended based on this study, is obtained with the fully *dependent* ($\rho=1$) simulations. In this case the sensor behaves identically with each inspection.

Effects of Changes in POD parameters

The effects of changing the COV and the median of the POD curve for independent and dependent inspections are shown in Figure 7. As the figure shows, it is possible to obtain a 100% CPOD even with fully dependent inspections. For this example the critical defect size is approximately 15.24 mm (600 mils). Thus, if the median of the POD is lower than the critical defect size and the COV is small enough such that the entire distribution is contained below the critical defect size, the flaw will always be detected. With a median value of 15.24 mm (600 mils), Figure 7 indicates that the CPOD at failure (1978 cycles) will be 0.5 regardless of the COV value.

Comparison of Depot Inspection versus Continual Inspection

A single but precise mid-life inspection is compared to a less-precise continual inspection. The issue under study is whether the use of continual monitoring will provide advantages over present day “depot” inspections. Figure 8 shows the normalized POF versus flight cycles (the results are normalized to the POF without inspection at 8000 flight cycles) considering: a) no inspection, b) a single mid-life inspection with a median POD value of 0.762 mm (30 mils) and a COV of 32%, c) continual inspections (once per flight) with a median POD value of 5.080 mm (200 mils) and a COV of 32%, d) continual inspections with a median POD value of 10.16 mm (400 mils) and a COV of 32%, e) continual inspections with a median POD value of 15.24 mm (600 mils) and a COV of 32%.

Figure 8 demonstrates that a single mid-life inspection reduces the POF to approximately 22% relative to the POF without inspection and effectively detects almost all defects that could cause fracture within the ensuing 4000 flight cycles. Continual inspections with a sensor that exhibits a POD of median value equal to 5.080 mm (200 mils) and a COV equal to 32% is far superior than a single more precise mid-life inspection, reducing the POF to near zero even though the precision of the on-board sensor is far less than the depot inspection.

Continual inspections with a sensor that exhibits a POD of median value equal to 10.16 mm (400 mils) and a COV equal to 32% reduces the POF to 11% relative to the POF without inspection. Continual inspection with this POD is still superior to a single more precise mid-life inspection through 8000 cycles although the slopes indicate that at some number of flight cycles the single mid-life inspection will be superior. Continual inspections with a sensor that exhibits a POD of median value equal to 15.24 mm (600 mils) and a COV equal to 32% reduces the POF to 50% relative to the POF without inspection and clearly is inferior to the single mid-life inspection. Table 2 summarizes the results. The results agree closely with Eq. (14).

Further confirmation of Equations 14 and 15 can be obtained by considering an analysis with four vastly different contrived POD curves developed such that $POD(a_{crit}) = 70\%$ for each curve, see Figure 9. In this case $P_{F, reduced} = 1 - POD(a_{crit}) = 30\%$ for each POD curve. The POD curves are not actual POD curves but only constructed to illustrate a concept. Table 2 shows the expected results ($P_{F, reduced}^{Theoretical}$), based on Equation 14, and computed results ($P_{F, reduced}^{Actual}$) based on Monte Carlo sampling with 20,000 samples and inspection after each flight. The numerical comparison at 8000 flight cycles is shown in Table 3. It is remarkable that the data indicate that all four POD curves predict the same reduced POF even though the POD curves are drastically different. These results verify Equations 13 and 14. These results are significant because they indicate that an estimate of the reduction in POF due to continual inspections can be ascertained by knowing the sensor's POD value at the critical defect size.

As an example problem, variations in stress scatter are considered with inspections with stress scatter modeled using a lognormal distribution; however, any distribution can be used. $P_{F, reduced}^{Actual}$ is determined using Monte Carlo sampling. To get the theoretical expected value, Equation 17 is evaluated between the limits of the pdfs. To facilitate this calculation, the $a_{crit} = f(\sigma)$ function is determined by developing a regression analysis (6th order), then developing the function $POD(a_{crit}(\sigma)) = POD(f(\sigma))$. Using these functions, Equation 17 was evaluated numerically for the case where stress scatter, and; therefore, a_{crit} , is a random variable.

Results from several different cases are summarized in Table 4. As indicated, the reduced POF is always greater than the theoretical value. Further, the difference between the expected and predicted value decreases as

the COV of the stress scatter decreases because the variation in a_{crit} decreases. As the COV of stress scatter goes to zero, a_{crit} becomes deterministic and the results converge to the values in the previous section.

Summary and Conclusions

During this research, a methodology was developed and implemented to compute the reduction in POF due to continual (once per flight) inspections based upon the concept of on-board crack sensors. A critical outcome of the research is that accurate Monte Carlo simulation of continual inspections requires that samples be generated as “dependent” across inspections. This modeling approach alleviates the substantial over prediction of sensor efficacy generated using the traditional assumption of independent inspections. Failure to do so results in much higher and unconservative estimates of POF reduction due to continual inspections. Mathematical bounds specify that the cases of dependent and independent inspections bound the cumulative probability of detection with dependent being most conservative and independent being the least conservative. If correlation between inspections is to be considered, the sum-of-uniforms method is ideal.

Numerical examples demonstrate the large differences that occur in cumulative probability of detection when comparing the results from dependent and independent inspections. After many inspections, say thousands, the differences can be orders of magnitude.

A second critical outcome is that the reduction in POF obtained by continual inspections depends almost solely upon the probability of detection of the sensor at the critical crack size, i.e., how reliably can the sensor detect the critical crack size. This information can be used to determine the required accuracy for an on-board sensor to prove effective. A straightforward expected value operation can be used for situations where the critical crack size is non-deterministic. This observation is borne out by the comparison of the reduction in POF by continual inspections versus a single, more accurate mid-life inspection. Continual inspections may be more effective than the accurate but single mid-life inspection if the continual monitoring system’s POD is sufficiently reliable at the critical crack size. Further collaboration is obtained from the analyses of four drastically different POD curves that all have the same POD value at the critical crack size. The results from the analyses are in effect the same.

The ability to correlate the reduction in POF to a simple measure such as the POD at the critical crack size is a major step in being able to determine the required sensitivity of a crack sensor to be beneficial. The consistency of $POD(a_{crit})$ in determining the reduction in POF depends somewhat on the steepness or flatness of the POD curve within a region around a_{crit} with a flatter curve being less sensitive to variations in a_{crit} . Even for a steep POD; however, $POD(a_{crit})$ still provides an excellent metric for determining the required accuracy of a sensor.

The issue of on-board inspections was investigated through the analysis of fracture of a gas turbine disk. However, the major conclusions are independent of structural component and are applicable to any other structural system that would benefit from on-board crack sensors such as off-shore structures, aircraft, automotive, refinery, nuclear structures, etc.

Notation

a	- crack size
a_{crit}	- critical crack size that fractures the material (load and material dependent)
$^n a_{DCS}$	- detectible crack size for a realization n of an inspection system
$^n a_{DCS(k)}$	- detectible crack size for a realization n for inspection k
a_{1-k}	- crack sizes from inspections 1 through k
a_k	- crack size at inspection k (estimated by fracture mechanics algorithms)
a_{last}	- crack size at the last inspection of a continual monitoring system
a_{kMi}	- crack size at inspection k minus i
COV	- coefficient of variation of lognormal POD function
$CPOD$	- cumulative probability-of-detection
$E[.]$	- expected value operator
f_{σ}	- probability density function of stress scatter random variable
f_{K_c}	- probability density function of fracture toughness

K_C	- fracture toughness random variable
M	- number of flight cycles
N	- number of Monte Carlo samples
$N_{f,woi}$	- number of samples that have failed without inspection
$N_{f,wi}$	- number of samples that have failed with inspection
POD	- probability-of-detection
POF	- probability-of-fracture
$P_{F,woi}$	- probability-of-fracture without inspections
$P_{F,wi}$	- probability-of-fracture with inspections
$P_{F,reduced}$	- ratio of the POF with inspection and the POF without inspection
$P_{F,reduced}^{Actual}$	- actual realized reduced POF due to inspection
$P_{F,reduced}^{Theoretical}$	- theoretical reduced POF due to inspection
nS_k	- $U(0,1)$ random number representing $POD({}^na_{DCS})$ for realization n
SOU	- sum-of-uniforms method
$U(0,1)$	- uniform random number with range zero to one
\tilde{X}	- median of lognormal POD function
ρ_{ik}	- correlation coefficient between a realization of nS_1 and nS_k
Φ	- standard normal operator
σ	- stress scatter random variable
σ_y	- standard deviation of the lognormal POD function

Acknowledgments

This work was supported under Air Force Agreement No. F33615-03-2-5203, Dr. Patrick J. Golden, AFRL/MLLMN, Project Monitor, and a subcontract with Southwest Research Institute, Dr. Stephen Hudak Jr., Program Manager.

References

- 1) Berens, A.P., Hovey, P.W., and D.A. Skinn, "Risk Analysis for Aging Aircraft, Vol 1-Analysis," Flight Dynamics Directorate, Wright laboratory, Wright-Patterson AFB, OH, WL-TR-91-3066, 1991.
- 2) Berens, A.P., "Nondestructive Evaluation and Quality Control," *Metals Handbook*, 9th ed., Vol. 17, pp. 689-701.1989
- 3) Chen, J., "Using the Sum-Of-Uniforms Method to Generate Correlated Random Variates with Certain Marginal Distribution," *European Journal of Operational Research*, Vol. 167, 2005, pp. 226-242.
- 4) Cornell, C. A., "Bounds on the Reliability of Structural Systems," *J. Structural Div., ASCE*, **93**, 1967.
- 5) DARPA News Release, "Prognosis Program Begins,"
<http://www.arpa.mil/body/news/2003/prognosis.pdf> December 3, 2003
- 6) Christodoulou, L. and J.M. Larsen, "Using Materials Prognosis to Maximize the Utilization Potential of Complex Mechanical Systems," *Journal of Metals, TMS*, March 2004, pp. 15-19.
- 7) Erland, K. "Quantifying the Benefit of Redundant Fluorescent Penetrant Inspection," *Review of Progress in Quantitative Nondestructive Evaluation*, Vol. 8B, 1988, pp. 2221-2228.
- 8) Grandt, A.F., Jr., "Fundamentals of Structural Integrity, Damage Tolerant Design and Nondestructive Evaluation," J. Wiley and Sons, Inc. 2004.
- 9) Harris, D. O., Dedhia, D. D., and Lu, S. C. (1992), "Theoretical and User's Manual for pc-PRAISE" Report No. NUREG/CR-5864. Washington, D. C.: Nuclear Regulatory Commission.
- 10) Hudak, S. J., Jr., Lanning, B. R., Light, G. M., Major, J. M. Moryl, J. A., Enright, M. P., McClung, R. C., and H. R. Millwater, "The Influence of Uncertainty in Usage and Fatigue Damage Sensing on Turbine Engine Prognosis, *Journal of TMS*, Nov. 2004.
- 11) Joly, R. B., Ogaji, S. O. T., Singh, R., and Probert, S.D., "Gas-Turbine Diagnostics Using Artificial Neural-Networks for a High Bypass Ratio Military Turbofan Engine," *Applied Energy*, Vol, 78, Issue 4, August 2004, pp. 397-418.
- 12) Larsen, J.M. and L. Christodoulou, "Integrated Damage State Awareness and Mechanism-Based Prediction," *Journal of Metals, TMS*, March 2004, p. 14.

- 13) Leverant, G. R., McClung, R. C., Millwater, H. R., and Enright, M. P., "A New Tool for Design and Certification of Aircraft Turbine Rotors", *Journal of Engineering for Gas Turbines and Power*, ASME, Vol. 126, No. 1, 2003, pp. 155-159.
- 14) Li, Y. G., "Performance-Analysis-Based Gas Turbine Diagnostics: A Review," *Proceedings of the Institution of Mechanical Engineers. Part A, Journal of Power and Energy*, Vol. 216, pp. 363-377.
- 15) Millwater, H.R., and P. Wirsching - "Analysis Methods for Probabilistic Life Assessment", *American Society of Metals Failure Analysis Handbook*, V 11, 2003, pp. 250-268.
- 16) "Nondestructive Evaluation System Reliability Assessment," *Department of Defense Handbook*, MIL-HDBK-1823, April 1999.
- 17) Rajesh, S. N., Udpa, L., and Udpa, S. S., "Estimation of Eddy Current Probability of Detection (POD) Using Finite Element Method," *Review of Progress in Quantitative Nondestructive Evaluation*, Vol. 12, 1993, pp. 2365-2372.
- 18) Shook, B. D., Millwater, H. R., Enright, M. P., Hudak, S. J., and Francis, W. L., "Impact of Multiple On-Board Inspections on Cumulative Probability of Detection," *ASME Turbo Expo*, GT2005-68585, Reno-Tahoe June 2005.
- 19) Shook, B. D., Millwater, H. R., Enright, M. P., Hudak, S. J., and Francis, W. L., "Comparison of Continual On-Board Inspections to a Single Mid-Life Inspection for Gas Turbine Engine Disks," *AIAA Conference*, Austin, TX April 2005.
- 20) Simola, K., and Pulkkinen, U., "Models for Nondestructive Inspection Data," *Reliability Engineering and System Safety*, Vol. 60, April 1998, pp. 112.
- 21) Simonen, F.A., Johnson, K.I., Liebetrau, A.M., Engel, D.W., and Simonen, E.P., "VISA-II A Computer Code for Predicting the Probability of Reactor Pressure Vessel Failure," *NUREG/CR-4486*, PNL-5775 (March 1986)
- 22) Southwest Research Institute, Turbine Rotor Material Design, Final Report, DOT/FAA/AR-00/64, Office of Aviation Research, Washington, D.C. December 2000

- 23) Thompson, B., Model-assisted POD Working Group,
<http://www.cnde.iastate.edu/research/MAPOD/Sept%202004%20Mtg/POD%20Workshop%20-%20Model%20Assisted%20POD%20-%20Sept%2023%2004%20-%20Thompson.pdf>, Feb. 2006
- 24) Willemain, T. R., and Desautels, P. A., “A Method to Generate Autocorrelated Uniform Random Numbers,” *Journal of Statistical Computation and Simulation*, Vol. 45, 1993, pp. 23-32.

List of Tables

Table 1 Example Problem Definition

Table 2 Predicted vs. Computed $P_{F, reduced}$ for Air-to-Ground Mission

Table 3 Predicted vs. Computed $P_{F, reduced}$ for Contrived POD Curves

Table 4 Predicted vs. Computed $P_{F, reduced}$ for Non-Deterministic Critical Crack Size

Property	Description	Comment
Loading	Spectrum loading representative of an Air-to-Ground mission	11600 time points, 231 load pairs
da/dN-ΔK	C=5.248E-11 (9.25E-13 SI), m=3.87, K _c =58.7 ksi-in ^{-1/2} (64.6 MPa-m ^{-1/2})	Paris law with no threshold (C – constant, m – exponent, K _c – fracture toughness) US – units: da/dN (in/cycle), ΔK (ksi-in ^{-1/2}) SI - units: da/dN (m/cycle), ΔK (MPa-m ^{-1/2})
Initial crack size	Probability distribution representative of crack at holes of compressor disks	Surface crack in the bore of a gas turbine disk. 1-1 aspect ratio
Propagation scatter	Median = 1, cov = 0.1	lognormal distribution – for all zones
Stress Scatter	Median = 1, cov = 0.1	lognormal distribution

Table 1 Example Problem Definition

POD Median ^a mil/mm	Expected %	Computed %
200/(0.508)	0.03	0.00
400/(1.016)	11.2	9.8
600/(1.524)	53.3	47.7

^aCOV constant at 32%

Table 2 Predicted vs. Computed $P_{F, reduced}$ from Air-to-Ground Mission

Median ^a		
mil/mm	Expected %	Computed %
200/(5.08)	30.0	30.0
400/(10.16)	29.9	33.6
500/(12.70)	30.0	33.7
600/(15.24)	30.1	33.8

^aCOV constant at 32%

Table 3 Predicted vs. Computed $P_{F, reduced}$ from Contrived POD Curves

POD Median mil/(mm)	Stress Scatter Median	Stress Scatter COV (%)	Expected POF Reduction (%)	Computed POF Reduction (%)
400/(10.16)	1	5	8.1	10.7
400/(10.16)	1	10	9.2	13.0
400/(10.16)	1.2	5	22.9	24.4
400/(10.16)	1.2	10	25.0	32.5
600/(15.24)	1	5	45.3	52.4
600/(15.24)	1	10	46.2	59.1
600/(15.24)	1.2	5	71.2	71.0
600/(15.24)	1.2	10	69.8	75.8

^aCOV constant at 32%

Table 4 Predicted vs. Computed $P_{F, reduced}$ for Non-Deterministic Critical Crack Size

List of Figures

1. Example POD curve
2. Single Inspection Simulation Schematic
3. Inspection Sampling Schematic for Independent Inspections
4. Inspection Sampling Schematic for Dependent Inspections
5. Effect of Critical Crack Size on Dependent Inspections
6. Effect of Inspection Correlation on Cumulative Probability of Detection
7. Effect of Variations in POD Parameters - Independent and Dependent Cases
8. Comparison of Continual and Single Mid-Life Inspection
9. Contrived POD Curves
10. Reduced POF Resulting from Contrived POD Curves

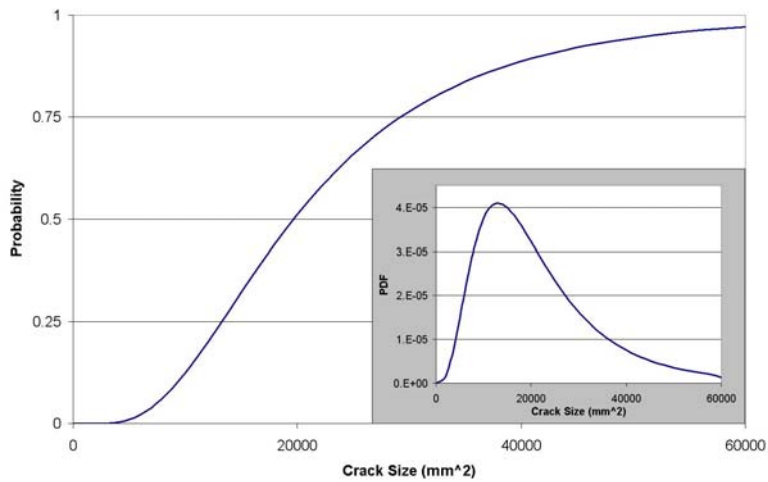


Figure 1 Example POD Curve

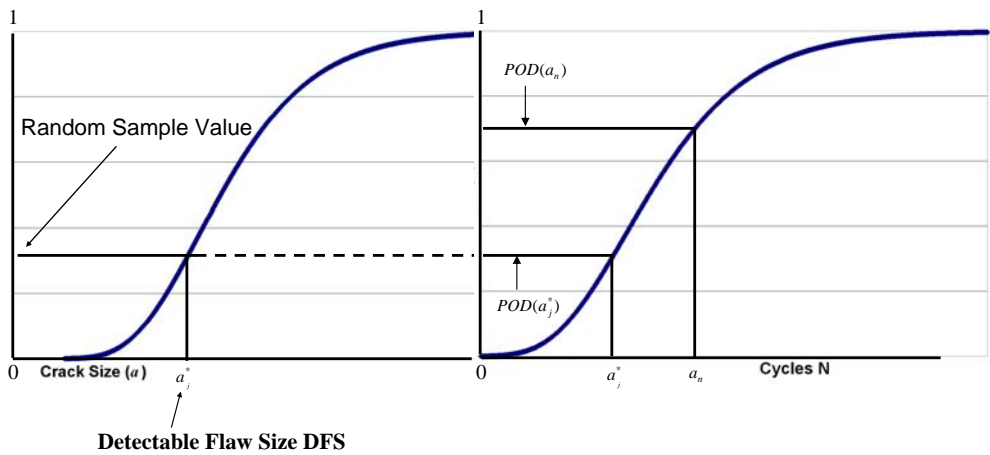


Fig 2 Single Inspection Simulation Schematic

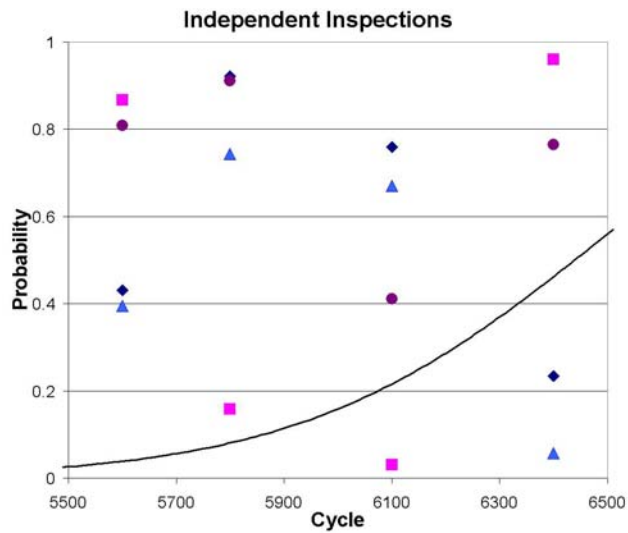


Fig 3 Inspection Sampling Schematic for Independent Inspections

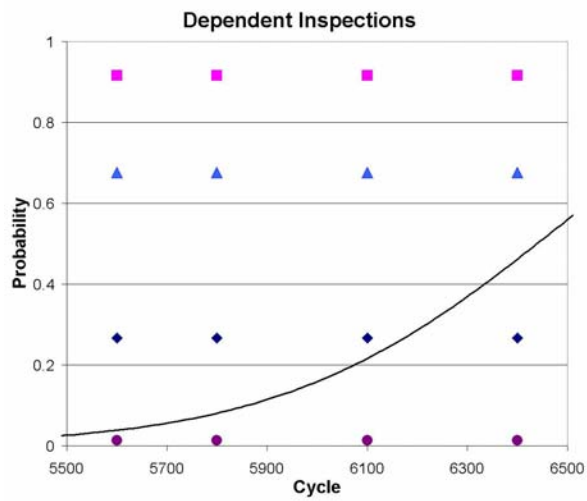


Figure 4 Inspection Sampling Schematic for Dependent Inspections

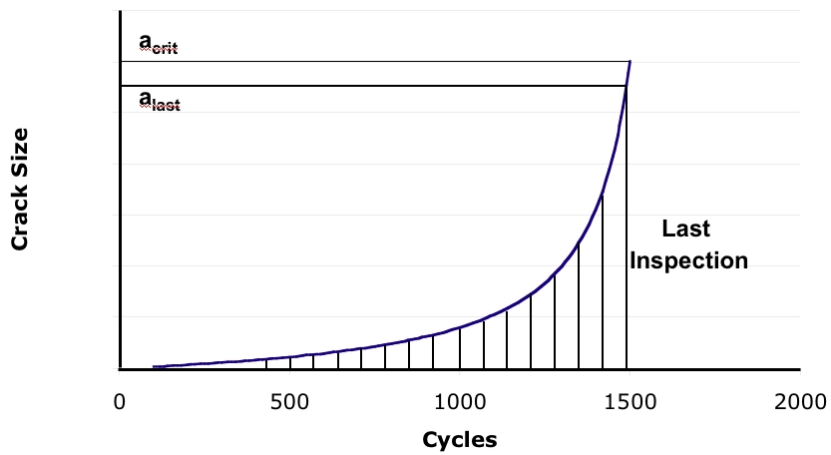


Fig 5 Effect of Critical Crack Size on Dependent Inspections

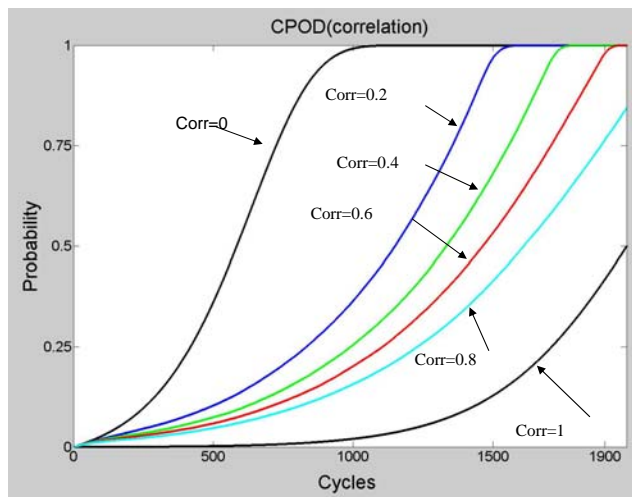


Figure 6 Effect of Inspection Correlation on Cumulative Probability of Detection

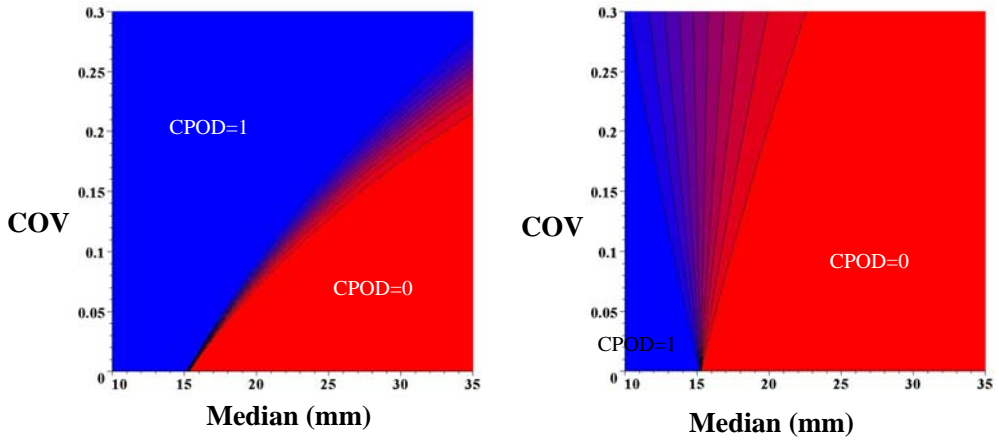


Figure 7 Effect of Variations in POD Parameters - Independent and Dependent Cases

7

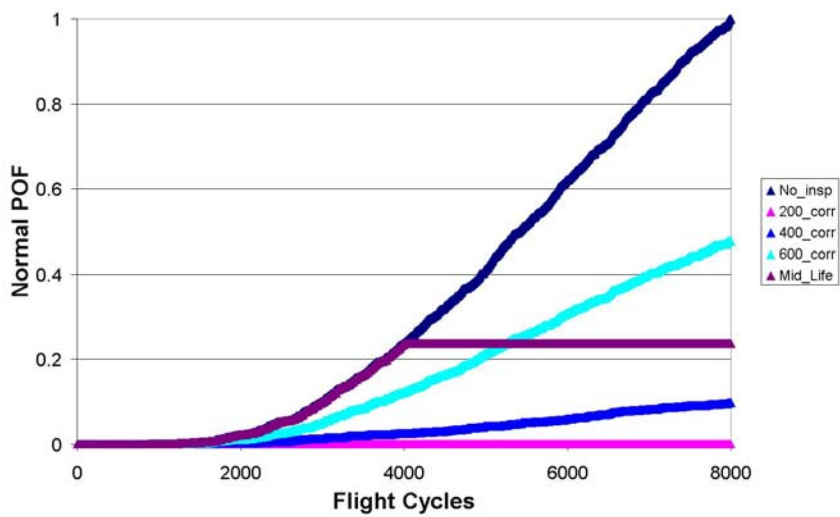


Figure 8 Comparison of Continual and Single Mid-Life Inspection

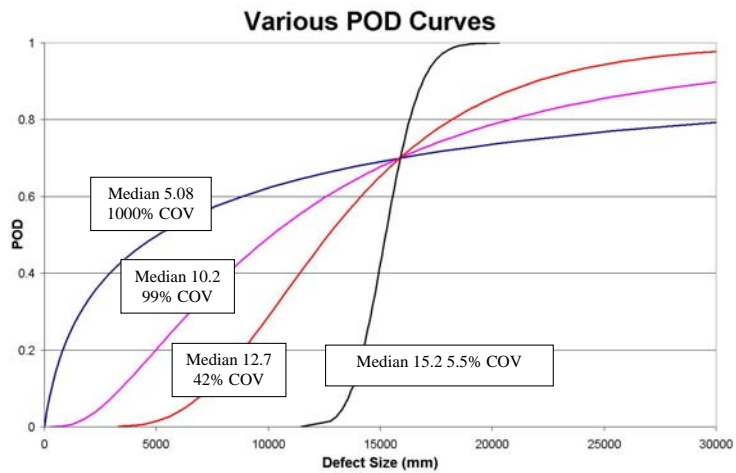


Figure 9 Contrived POD Curves

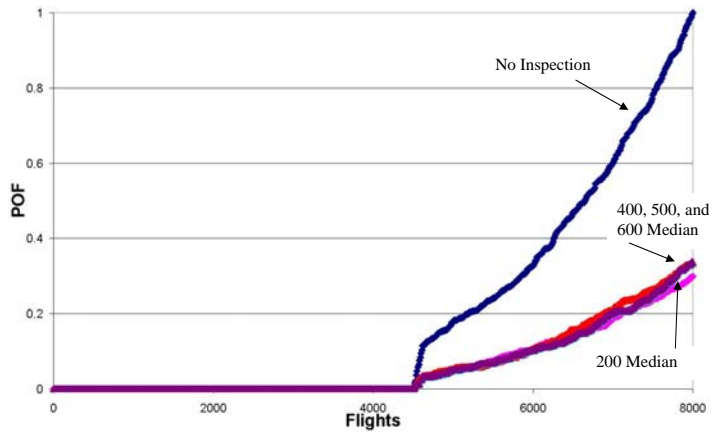


Figure 10 Reduced POF Resulting from Contrived POD Curves